IHJPAS. 37 (2) 2024
Ibn Al-Haitham Journal for Pure and Applied Sciences
Journal homepage: jih.uobaghdad.edu.iq
PISSN: 1609-4042, EISSN: 2521-3407

Synergistic Inhibitory Effect of Biosynthesized ZnO-CuO Nanocomposite on Biofilm Formation of *Proteus mirabilis*

Noor Hamza Faiq[1*] and Mais E. Ahmed[2]
[1,2] Department of Biology, College of Science, University of Baghdad, Baghdad, Iraq
*Corresponding Author.

Received 5 April 2023 Accepted 22 May 2023 Published 20 April 2024
doi.org/10.30526/37.2.3383

Abstract

Proteus mirabilis is considered the third most common cause of catheter-associated urinary tract infections. With urease production, the potency of the catheter's blockage due to the formation of biofilm is significantly enhanced. This study was aimed at exploring whether green synthesized ZnO-CuO nanoparticles (ZnO-CuO NPs) can function as an anti-biofilm agent produced by *P.Mirabilis*. The characterization of biosynthesized nanoparticles was carried out to determine the chemical and physical properties of the product using AFM, TEM, FESEM, XRD, and UV visible spectrometry. The hexagonal structure was confirmed by XRD, the size range was marked at 96.00nm by TEM, and FESEM was used to confirm the surface morphology. AFM analysis is used to reveal the roughness and distribution of nanoparticles. UV-visible spectra of the synthesized nanoparticles recorded a maximum peak at 287nm and 232nm. Zinc and Copper nanoparticles showed remarkable biofilm inhibitory effects on wild-type strains of multidrug-resistant *Proteus mirabilis*. Downregulation changes in *LuxS* expression using real-time PCR technology were detected after treatment with the ZnO-CuO nanocomposite of these strains. A cytotoxicity test of CuO-ZnO NPs-based nanocomposite showed that this nanocomposite is safe for use, where the IC_{50} was 161.6 µg/mL. Anti-cancer activity against urethral bladder cancer cell lines was recorded in vitro, where the IC_{50} was 107.4 µg/mL.

Keywords: Proteus mirabilis, anti- biofilm, Zinc oxide nanoparticles, Anti-cancer, copper oxide nanoparticles.

1. Introduction

Bacterial biofilms are well-organized communities with single or multi species enclosed by a defensive polysaccharide matrix containing extracellular DNA, lipids, and proteins [1]. The community of biofilm depends on complicated communications, enabling the pathogens to develop resistance against host defense mechanisms, different stress factors, and antibiotics [2]. Bacterial biofilms are ubiquitous in clinical settings since they can increase bacterial resistance up to 1000 fold in compression to planktonic cells. Subsequently, despite anticipation measures taken in hospitals and other clinical settings, nosocomial infections still result in major morbidity and mortality rates [3]. In this emerging situation, researchers are commended for improving new alternatives to traditional antibiotic treatment that can successfully combat multidrug resistance (MDR) and biofilm-producing bacteria.

The green synthesis of metal oxide NPs has gained great interest since it is a clean, eco-friendly approach and has a wide range of applications in the biotechnology and medical fields [4]. ZnO and CuO nanoparticles display variable shapes and sizes with a minimum surface area that allows them to penetrate microbial cells; therefore, they are considered powerful antibacterial agents against a wide range of bacterial species [5].

ZnO NPs are one of the most important nanoparticles of metal oxides; they are a unique and inorganic material that can be used in several biological applications (anti-bacterial, anti-inflammatory). Several studies have described the quorum sensing system as a potential target for antimicrobial agents that limit biofilm formation [6]. Researchers in recent years have employed nanotechnology to improve antimicrobials that can target virulence factors without disturbing mammalian cells. Metal NP synthesis using microorganisms has represented a novel alternative to chemical and physical approaches as antibacterial, antioxidant, and antifungal agents, along with anticancer properties, in many different applications [7].

Several studies were interested in investigating the antibacterial activity of CuO. Noor in 2020 revealed in her study a moderate antibacterial activity of fungal-mediated CuO NPs against *E.coli, K. pneumoniae*, and other gram-negative bacteria [8]. The anti-cancer activity of zinc nanoparticles was previously approved against HeLa cell lines in cervical cancer. Zinc NPs can induce apoptosis through ROS production inside cancer cells. Induced cell cycle arrest, decreased antioxidants, and increased lipid peroxidation were also observed [9].

2.Materials and methods

2.1.Sample collection

A total of 100 urine samples were collected from patients with urinary tract infections and resident hospital patients with urine catheters presented to the AL Yarmouk Teaching Hospital.

Isolation and identification: *P.mirabilis* was identified primarily by culturing on MacConkey and Blood agar at 37 °C for 24 h and confirmed by the VITIC 2 system.

2.2.Antibiotic susceptibility test

According to CLSI 2021, the susceptibility test takes place using the disk method on Mueller-Hinton agar plates. The antibiotics used were (Levofloxacin 5 µg, Ciprofloxacin 15 µg, Ampicillin 25 µg, Gentamicin 10 µg, Cefoxitin 30 µg, Ticarcilline + Clavulanic Acid µg, Piperacillin-Tazobactam 100/10 µg, Cefepime µg, Nitrofurnation 300 µg).

2.3.Nanocomposite preparation

As precursors, copper (II) acetate Cu (CH_3COO) $2{\cdot}H_2O$) and Zinc acetate (Zn ($O_2CCH_3)_2$) were used in this research.

2.4.Preparation of bacterial suspension

P. mirabilis was grown in 250 ml of Brain Heart broth at 37 °C for 24 hours in a non-shaking incubator. The bacterial broth was then centrifuged, the supernatant was collected, and the sediment was discarded.

2.5. Synthesis of CuO-ZnO NPs

The nanocomposites were synthesized by the precipitation method: (200ml) of *P. mirabilis* broth filtrate, 10 g of copper (II) acetate, and 10 g of Zinc acetate were added at room temperature (37 °C), sealed, and covered with a dark plastic bag, and then incubated in a shaker incubator for 24 h. The mixture was then centrifuged, and the precipitate was collected and washed thrice with deionized water. The nanoparticles were synthesized by the extracellular route, where metal ions get reduced on the cell surface by the action of bacterial reducing

enzymes. Next, NPs synthesis can be detected by the color change of the solution; the precipitant is then air dried and kept in a dry place for further characterization [10].

2.6.Characterization of CuO-ZnO nanocomposite

Characterization is essential for understanding nanoparticle properties. The following methods were used to determine the characteristics of NPs: for determining shapes and sizes, SEM and TEM were used. Atomic force microscopy (AFM) is used to define the height and volume of NPs in 3D vision, and UV-visible (UV-DRS) is used to study the optical properties of the samples. (XRD) is a technique used in materials science to determine the crystallographic structure of a material [11].

2.7.MIC determination

We used the broth microdilution method in Eppendorf tubes to figure out the minimum inhibitory concentration (MIC) and the lowest concentration of synthesized nanoparticles that stop bacterial growth. We prepared the bacterial inoculum in MHB and modified the concentration to 100 UFC/mL. Double serial dilutions of nanocomposite were prepared in (16, 32, 64,128, 256,and 512 µg/ml) using MHB in six tubes, which were then incubated for 24 hours at 37°C.

2.8.Quantitative determination of biofilm formation was determined by a colorimetric microtiter plate assay [12]**.**

1- Brain heart infusion Broth supplemented with an additional 1% glucose was used for this assay.

2-Biofilm inoculums for cultivation were made from bacteria cultivated in broth, diluted 1:100, and poured into the well with 200 µl. Only broth is used in the negative control wells (200 µl of BHI supplemented with 1% glucose per well). Each strain was tested in three different ways.

3- Under static conditions, the inoculated plate was covered with a lid and incubated aerobically for 24–30 hours at 35–37°C.

4- The contents of the wells were decanted, and each well was washed three times with (300 µl) of PBS (2.2.5.1). The plates were then drained, inverted, and fixed with 150 of ml methanol.

5- Staining was done with (150 µl) of crystal violet at room temperature for 15 min, then washed and dried at room temperature.

6- For dye re-solubilizing, 150 µl of 95 percent ethanol was added, and the microtiter plate was covered with the lid and left at room temperature for at least 30 min. without shaking.

7- Using a microtiter-plate reader (GloMax/ Promega-USA), the optical density (OD) of each well was measured at 630 nm, and the results were as follows:

$OD \leq ODc$ = no biofilm producer;

$ODc < OD \leq 2\ ODc$= weak biofilm producer;

$2\ ODc < OD \leq 4\ ODc$ = moderate biofilm producer;

$4\ ODc < OD$= strong biofilm producer

The cut-off value for the negative control is ODc, which is defined as three standard deviations (SD), above the mean OD of the negative control: ODc= average OD of negative control+ (3× SD of negative control).

2.9.Effect of CuO-ZnO nanocomposites on Biofilm formation

This assay was carried out on a 96-well microtiter plate, as performed by [13]. Tested isolates were cultured in brain-heart infusion broth at 37^{o} C for 24 h. 100 ml of bacterial inoculum was adjusted to 0.5 McFarland and added to each well. 100 ml of nanocomposite suspension was added to each well at the sub-inhibitory concentration, and the tubes were incubated at 37^{o} C for

48 h. A positive control was presented as bacterial culture without Nano formulations, while clear broth was considered a negative control. The contents of each well were discarded after incubation, and the microplate was rinsed thrice with sterile saline and dried for 45 minutes at 60 °C200 ml of 0.1% crystal violet were used in staining, followed by incubation at room temperature for 15 min. The microplate was rinsed three times with sterile normal saline. Then acetic acid at 30% was added to each well by 200 ml, and the optical density (OD) was read at 630 nm for all wells using a microtiter plate reader.

2.10. RT-qPCR protocol

The presence of *LuxS* and *rpo* in *P.mirabilis* was determined by employing the thermal cycler to amplify the isolated genomic DNA (Thermo Fisher Scientific, USA). This main step is separated into two stages. The first stage is the synthesis of cDNA from RNA using specific primers for LuxS and *rpo* transcripts, as mentioned in **Table 1.** and the proto-script cDNA synthesis kit. This procedure has been performed as detailed in the manufacturing procedure. The second stage of this protocol is done by taking cDNA samples from tested isolates and controls at the same time. For each sample, there are three PCR tubes, and one tube for the *LuxS* gene, *rpo,* which is considered a housekeeping gene in this study. The fluorescent power of Syber Green is used for quantity estimation. The reaction mix of components with their quantity is mentioned in **Table 1.** below:

Table 1. Synthesis of cDNA from RNA using primers for *LuxS, rpo* transcripts

Component	20 ul
Luna Universal Master Mix	10 ul
Forward primer	1 ul
Reverse primer	1 ul
Template DNA	5 ul
Nuclease-free Water	3 ul

The difference in cycle thresholds (Ct) and fold changes between the treated groups and the calibrators for each gene were evaluated [14]. The *rpo* values were used to normalize the data. PCR tubes were spanned and the liquid was collected for 1 minute at 2000g, then the program for real-time PCR was setup with the indicated thermos cycling protocol. The result was collected and analyzed by the Livak formula. Relative quantitation was used to determine expression levels.

2.11. Anti-cancer activity of CuO-ZnO nanocomposite

2.11.1. Determination of Cell Viability

The cytotoxic effect of CuO/ZnO NPs synthesis from *P. mirabilis* was performed by using MTT ready-to-use kit contents [15], UBC-40, and HdFn cell lines in 96-well microtiter plates at a concentration of 4000 cells per well. After 12 hours of incubation, the growth medium was replaced with a fresh medium containing various concentrations of nanocomposite (25, 50, 100, 200, and 400 μg/ml) to treat both cell lines. According to the provider's instructions, the cells were cultured with the recommended medium at 37 °C. A microplate reader from Bio-Tek, Georgia, USA, was used to detect absorbance at 450 nm. Curves were generated with GraphPad Prism 7 software from GraphPad Software, Inc., USA, in a dose-dependent manner.

3.Results and discussion

3.1. Isolation and identification:

Out of 100, 46 isolates were confirmed as *P. mirabilis*, the conformation was carried out by the VITEK 2 system, which was considered a reliable identification by Biochemical tests; in addition, swarming on blood agar as shown in **Figure 1**. and colony morphology on MacConkey agar.

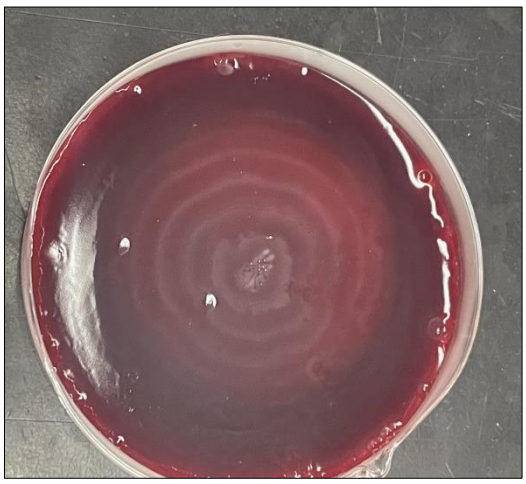

Figure 1. *Proteus mirabilis* on blood agar at 37C for 24h of incubation.

3.2. Antibiotic susceptibility test

3.2.1. MDR strains screen:

Forty out of sixty-four isolates (62.5%) were confirmed as MDR strains. After incubation at 37 °C for 24 hours, all tested isolates were resistant to Piperacillin-Tazobactam, six isolates (15%) were only resistant to levofloxacin; while six isolates (15%) were found to be resistant to ciprofloxacin; ampicillin did not inhibit the growth of 15 isolates (37.5%); gentamicin resistance was found in two strains only (5%); six isolates (15%) were recorded as cefoxitin resistant; and 17 isolates (42.5%) were resistant to nitrofurantoin. A ten-year study in 2019 shows a growing concern about antibiotic resistance in proteae (the proteae tribe includes the genera *Proteus*, *Morganella* and *Providencia*) Based on the results of the study, Resistance rates to third-generation cephalosporins developed significantly (the indicator during the study was ceftriaxone). Resistance to Ceftriaxone has increased by three times in hospitalized patient samples [15]. Another study carried out in China stated that 25 isolates of 54 *P. mirabilis* were classified as MDR. The samples were collected from animals and humans. This study highlighted that *P. mirabilis* produces AmpC β-lactamases and extended spectrum β-lactamases, which makes this bacterium a serious public health risk. *P. mirabilis* uses an efflux pump to resist the main classes of antibiotics [16].

3.3. Biosynthesis of ZnO-CuO Nanoparticles

Zinc oxide nanoparticles were biosynthesized from *P. mirabilis*. The formation of Nanoparticles was indicated by a color change from yellow to blue, in addition to forming a light blue precipitate. After centrifugation, the precipitate appeared in a greenish-blue color. After drying with the microwave, we obtained a shiny blue powder, as shown in **Figure 2**. In recent years, an obvious coordination to use bacteria to synthesize nanomaterials (mainly silver, zinc, gold, and nanoparticles) with remarkable properties has been observed for the development of antimicrobials with in vitro activities against pathogenic bacteria [17]. Bacteria are easy-

cultivating microorganisms with short generation times; these characteristics make bacteria a great candidate for nanoparticle synthesis as they have extra cellular reduction enzymes [18]. The anti-biofilm activity of zinc oxide NPs was previously reported on *S. aureus* and *P. aeruginosa* [19].

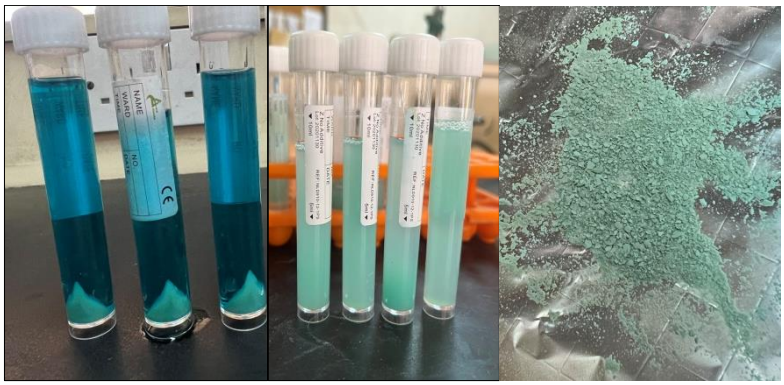

Figure2. Biosynthesis of CuO-ZnO Nanocomposite Powder

3.4. Characterization of Nanocomposite

3.4.1. UV–Vis Spectral Analysis

For this typical analysis, the sample was dissolved in deionized water. The results confirmed the formation of freshly prepared ZnO and CuO. Biosynthesized CuO-ZnO NPs exhibited absorption peaks at 287nm and 232 nm, as shown in **Figure 3**. Two peaks were detected, representing the presence of zinc oxide and copper oxide, as reported by [20].

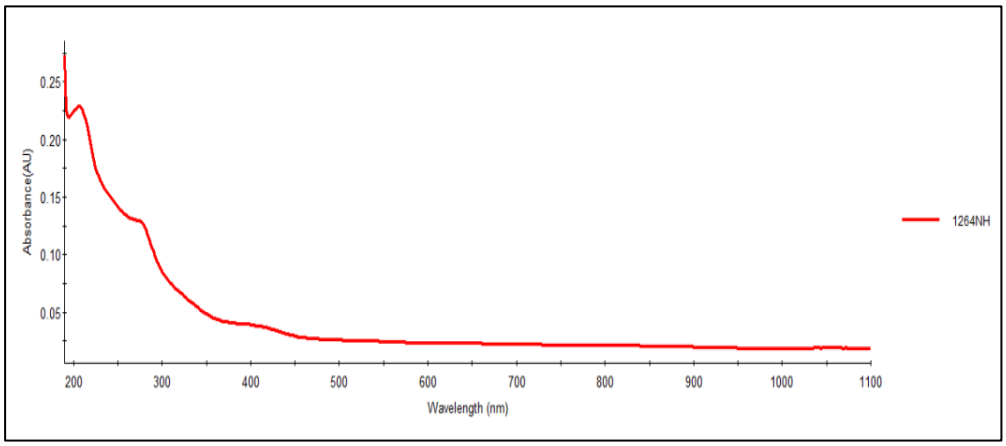

Figure 3. UV visible of nanocomposite.

3.4.2. Atomic Force Microscopy (AFM) analysis

AFM analysis of CuO-ZnO NPs was performed with CSPM to identify and characterize the distributions of nanoparticles. The estimated grain size and mean square roughness were determined. As shown in **Figure 4**. Portraits of a three-dimensional profile of nanocomposite and a 3D image of the nanoparticles show that the average grain size is 96.00nm. Different magnification ranges were conducted to give an insight into the roughness and topography of nanoparticles at 1.93 µm, 3.3 µm, and 3.46 µm.

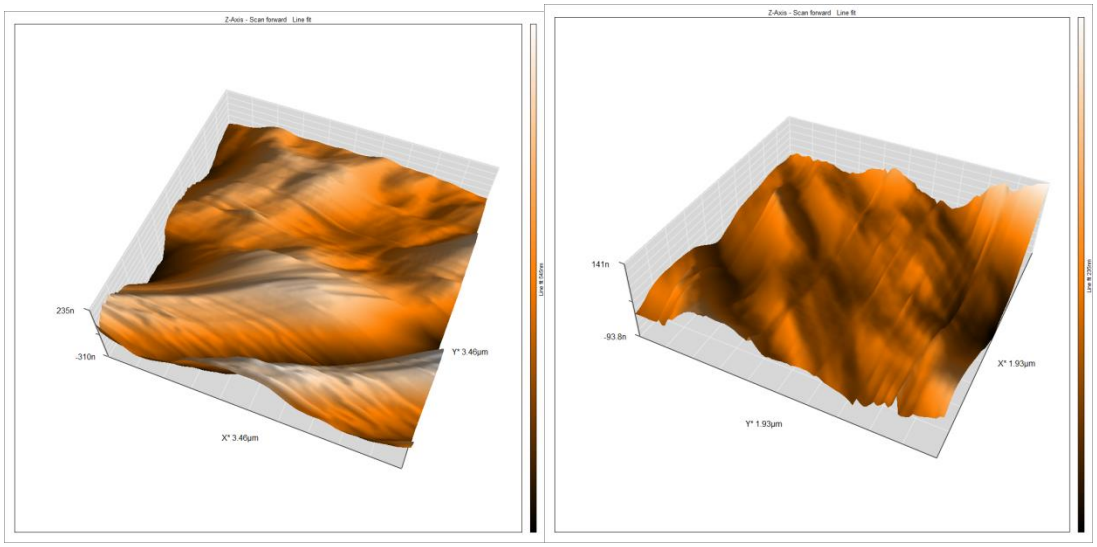

Figure 4. Atomic Force Microscopy analysis of CuO-ZnO nanocomposite.

3.4.3. Transmission Electron Microscopy analysis (TEM)

TEM imaging was used to explore the morphology and size of the nanocomposite. The core structure of the nanoparticles is confirmed by TEM analysis [21]. TEM images in **Figure 5.** demonstrate the formation of spherical and semi-spherical-shaped particles with agglomeration. The TEM images show that CuO-ZnO NPs, formed by the reduction of copper and zinc ions using *P. mirabilis* Filtrate, are spherical . Metallic nanoparticles are well protected against chemical oxidation by the organic shell of bacterial growth medium, which makes them constant and suitable for coatings or biotechnology applications [22]. These results are consistent with those of FESEM and XRD studies.

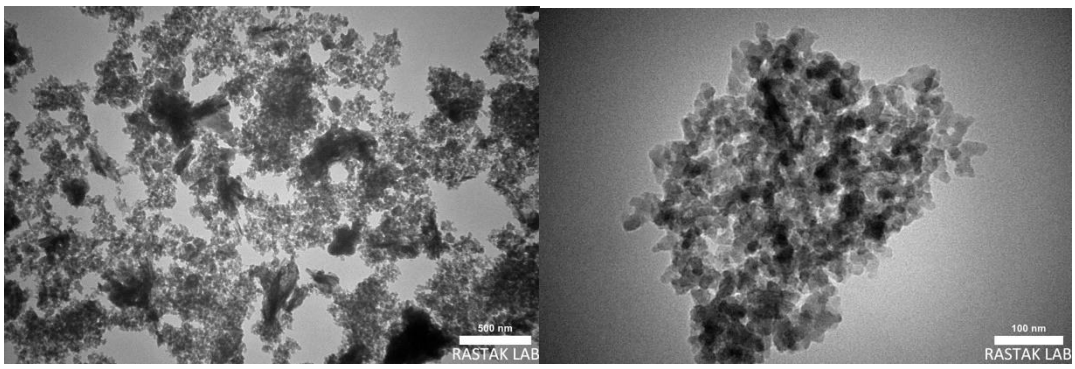

Figure 5. The Transmission Electron Microscopic TEM images of CuO-ZnO NPs

3.4.4. Scanning electron microscopy SEM

Scanning electron microscopy (SEM) provided further insight into the surface morphology of the Cu-Zn NPs. Images reveal that CuO-ZnO NPs are crowded together to look like combined cauliflower **Figure 6**. Higher magnification for further observations reveals that these crowded NPs are groups of smaller nanoparticles of copper and zinc that exhibit spherical-shaped structures with good homogeneity.

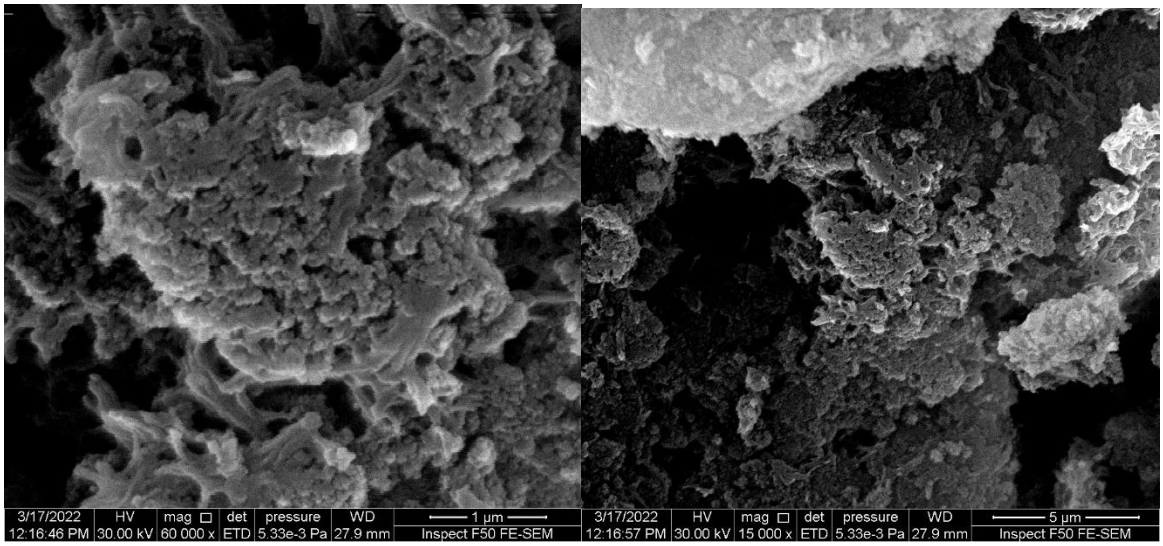

Figure 6. FESEM images with 60000x and 15000x magnification powers.

3.4.5. X-ray Diffraction (XRD)

The crystalline structure and purity of synthesized nanoparticles (NPs) have been investigated with the help of dispersive X-ray diffraction. The XRD spectra of Cu-Zn NPs powder are shown in **Figure 7**. which confirms the presence of Cu-Zn NPs by revealing 19 prominent peaks that correspond to the diffraction peaks at 2θ values: 11.794, 13.056, 16.766, 18.12, 19.525, 20.539, 22.494, 24.312, 35.725, 39.148, 42.864, 54.37, 57.254, 58.473, 59.689, 61.492, 72.206, 73.681, and 77.314. According to JCPDS file No. 79-0207, all peaks have been indexed via the wurtzite hexagonal phase. No peaks were present in the spectrum related to any impurities or bulk remnant materials detected except the characteristic peaks related to the wurtzite hexagonal phase of CuO-ZnO, indicating the high purity of synthesized uncapped NPs.

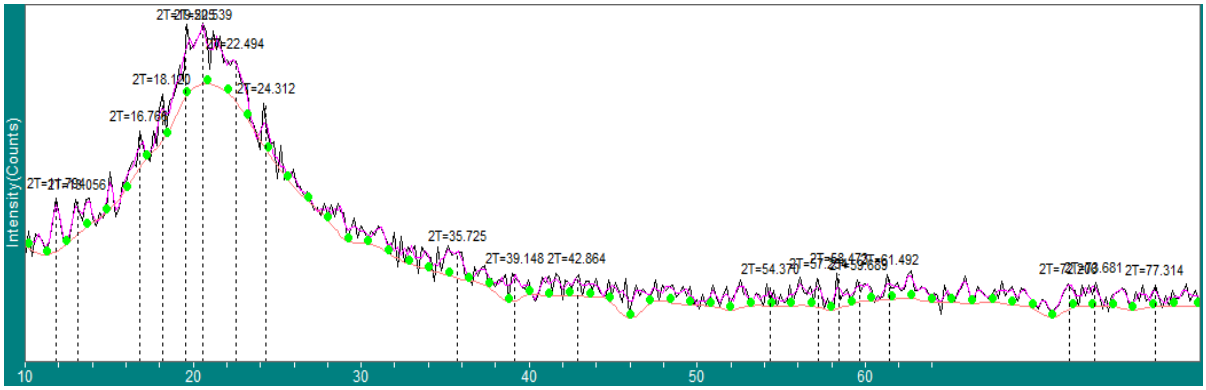

Figure 7. X-ray Diffraction XRD of nanocomposite shows 19 peaks at 2θ values.

3.5. Determination of biofilm formation before treatment with Nanocomposite

A total of 20 MDR isolates were tested for their biofilm production ability using a plastic micro titer plate; nine isolates were recorded as strong biofilm producers, as detailed in **Figure 8** and **Table 2**. To estimate the effect of Cu-Zn NPs on the biofilm production of these isolates, five strong producers' strains were selected. The OD of each well was read at 630 nm using a micro titer plate reader.

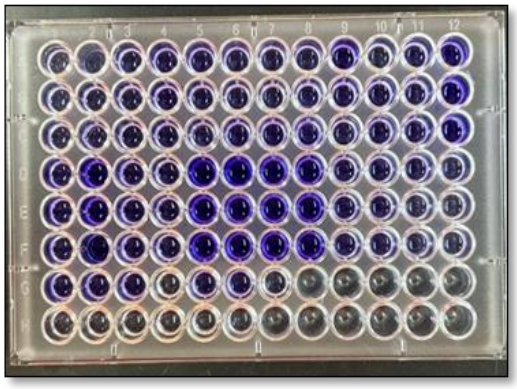

Figure 8. Micro titer plate assay for biofilm production

3.6. Determination of biofilm formation after treatment with Nanocomposite

Biofilm production was significantly reduced after 48 hours of incubation at 37 °C with a sub-MIC of Cu-Zn NPs. The OD measurement of the same nine strains of *P. mirabilis* lowered from strong to weak production, as detailed in **Table 2.** and **Figure 9**.

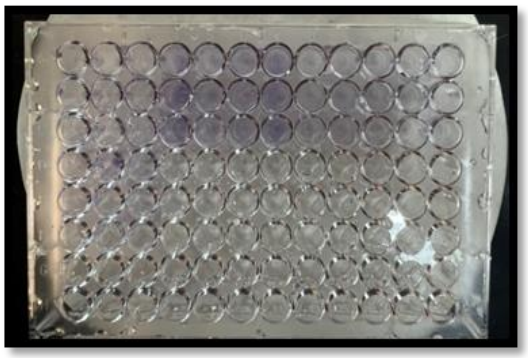

Figure 9. Microtiter plate assay for biofilm production after treatment with CuO-ZnO NPs Sub MIC

Table 2. O.D values before and after treatment with biogenic CuO- ZnO.

NO. of isolate	O.D Before treatment	O.D after treatment with CuO-ZnO NPs
1.	5.75	1.0
2.	9.19	1.45
3.	6.30	1.11
4.	7.25	1.14
5.	7.15	1.17

Antimicrobial action can be explained by the small particle size of ZnO NPs because smaller materials can enter bacterial cell membranes and cause cell damage. The anti-biofilm activity of zinc oxide NPs was previously reported in several studies; one study showed a significant decrease in the biofilm formation of pseudomonas aeruginosa after treatment with zinc oxide NPs in a concentration-dependent manner [23]. Biofilm formation is considered a target for different antimicrobial agents, such as nanoparticles from different sources and silver NPs synthesized from Date palm extract against E. coli and *Klebsiella pneumonia* [24]. This study also agreed with other studies that approved the Anti-biofilm activity against methicillin resistant Staphylococcus Aureus [24]. This action can be explained by the ROS generated by nanoparticles that impose oxidative stress, causing bacterial cell destruction [25]. Studies also found that treatment with nanomaterials induced a major reduction in membrane potential, signifying it may target the membranes of bacterial cells [26].

3.7. Gene expression of *LuxS*

LuxS is a transcript of the structural operon luxCDABF that is responsible for the production of autoinducer 2 AI-2, which predominantly participates in cell-to-cell signaling in bacteria. The transcription of *luxS* is enhanced when *luxR* is bound to an autoinducer. After *luxS was* produced, AI-2 cast signals that were used to sense interspecies interaction and its cell density in multi-microbial populations that have essential roles in the regulation of virulence factors [27]. RT-PCR reveals a major downregulation in *LuxS* expression after exposure to CuO-ZnO NPs suspension compared to normal gene expression in bacterial broth with no NPs involved, as detailed in **Table 3**. A fold change in gene expression reveals that *LuxS* was down-regulated in response to copper oxide and zinc oxide NPs in three out of five isolates of *proteus mirabilis;* the other two isolates were almost not affected, as entailed in **Table 3**.

This result corresponds with the phenotypic changes in biofilm formation in the microtiter plate experiment carried out in this study, as shown in **Figure 10.** above. This finding was accepted with other reports by Rajalakshmi and Sangeetha [28]. The anti-biofilm activity of metal oxide nanoparticles has gained great interest in the last few decades since biofilm is an important virulence factor that enables bacteria to resist antibiotics [29]. Several studies have approved that these particles have bactericidal and bacteriostatic activity. Khan *et al*. confirm the downregulation effect of ZnO NPs on *las* and *pqs* systems that control quorum sensing and biofilm production in *P. aeruginosa* [30]. Other reports estimate the ability of Nano oxides to inhibit QS systems of *S. agalactiae* [31].

Table 3. Ct before and after treatment with CuO-ZnO.

Ct before treatment with CuO-ZnO NPs				**Ct after treatment with CuO-ZnO NPs**				
Isolate No.	**Ct *rpo***	**Ct *LuxS***	**ΔCt**	**Ct *rpo***	**Ct *LuxS***	**ΔCt**	**ΔΔCt**	**Fold Change**
P.1A	13.73	12.32	-1.41	12.59	12.31	-0.28	1.13	0.456
P.2B	13.77	11.75	-2.02	16.75	17.05	-0.3	1.72	0.303
P.3C	10.91	12.4	-1.49	11.01	11.68	-0.67	0.82	0.566
P.4D	11.03	11.67	0.64	11.96	10.89	-1.12	-1.76	0.29
P.5E	10.31	10.47	0.16	12.66	12.06	-0.6	-0.76	1.693

The effect of metal-based nanoparticles depends on particle size, morphology, and composition. Dispersion, aggregation, or agglomeration also play a key role in the nanoparticle effect [32]. Most studies attributed the effect of zinc oxide NPs on the quorum sensing system to signal perception and response rather than the synthesis of autoinducers [33]. Other reports revealed the effect of polymeric nanoformulations on the attachment of biofilm cells to *Pseudomonas aeruginosa* (PAO1) [34]. Our results demonstrate that Cu-Zn NPs exhibit selective toxicity towards prokaryotic cells, prompting further investigation into NP toxicity in eukaryotic cells.

3.8. Cytotoxic effect of CuO-ZnO nanocomposite

Human Dermal Fibroblasts, neonatal (HDFn) cell line used to measure the cytotoxic effect viability, were reduced to half after treatment with the nanocomposite (161.6 mg/L IC50). **Figure 10.** shows cell viability getting lower with the nanocomposite concentration increment. The cytotoxic effect of copper nanoparticles generally depends on their physicochemical properties, including particle shape, size, aggregation, crystallinity, and surface coating. Reports have been recorded to be ten times lower than the toxic dose of ionic copper and copper (I) oxide

CuO to some plants, rodents, and cell cultures, thus classifying it as more cytotoxic. This fact can be exploited by proposing the use of copper nanoparticles as a drug carrier in chemotherapy [35]. Several studies take place to estimate the toxic effect of nanoparticles on human cells. There is a significant decrease in the human T cell count after treatment with ZnO NP; 77% of the cells remain viable at 5 mM, and 43% are kept at 10 mm. [36]. On the other hand, copper toxicity has been under investigation in the last few years. Neurodegenerative disorders, including Alzheimer's and Parkinson's diseases, have been linked to copper toxicity. Wilson and Menken diseases are also labeled as copper intolerance examples [37]. The nanoparticle interaction can also cause inflammation in tissues, oxidative stress, and histopathological lesions [38].

3.9. Anti-cancer activity of CuO-ZnO nanocomposite

Urethra bladder cancer cells used in this research show reduced viability after treatment with CuO-ZnO nanoparticles in dose-dependent matter. As **Figure 10.** clarifies, the IC50 value of nanocomposite that inhibits cell line viability is 107.4 mg/l. According to the data collected by this test, cancer cell viability was much lower than HdFn cells in the same concentrations. This leads to the conclusion that CuO-ZnO nanocomposite had a greater effect on cancer cells. The anti-cancer activity of nanoparticles was extensively studied to estimate the capability of nanoparticles to act as anti-cancer agents in humans and animals. Apoptosis is the most frequently mentioned model of cell death after exposure to metal-based nanoparticles; the second model is necrosis, with approximately half as much. The third path of nanoparticle cytotoxicity in cancer cells is also reported, and it involves the stimulation of autophagy, in which cell organelles and proteins are degraded. In one study recorded using MTT, apoptosis, and gene expression methods, nanoparticles with a 30nm size were found to have more anti-cancer potential than 60 nm CuO NPs against the 4T1 cell line as malignant breast cancer cells. [39]. Another study revealed the significant role of CuO NPs in inhibiting TIC-enriched PANC1 human pancreatic cancer cell cultures [40]. On the other hand, Zinc Oxide NPs were also under investigation as anti-cancer material. The human melanoma cell line (A375) was used to estimate this role in one study. The mRNA expression of apoptotic genes like caspase 3, 8, and 9 was elevated, followed by exposure to ZnO. Nanoparticles also stimulate apoptotic cell necrosis at the transcriptional stage [41]. Other results showed the effect of zinc oxide on cancer cell lines and toxicity assays [42]. The genotoxic effect of nanoparticles on cancer cells was also investigated. The suggested mechanisms of action that cause cellular damage by nanoparticles are Oxidative stress, ROS generation, and reducing mitochondrial membrane potential [41].

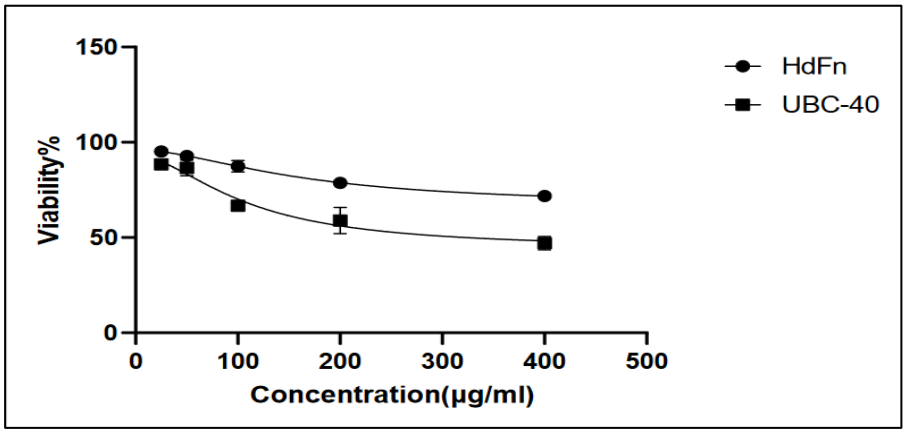

Figure 10. The IC50 value of nanocomposite that inhibits cell line viability

4. Conclusions

CuO-ZnO NPs were successfully synthesized following a direct, eco-friendly, low-cost, high-yield, and green method. CuO-ZnO NPs showed exceptional antimicrobial activity against several bacterial strains. Thus, NPs can be used for external purposes as antibacterial agents by coating surfaces on various substrates to prevent biofilm-producing microorganisms from attaching and colonizing in indwelling medical devices. The application of nanoparticles is increasing nowadays due to their effectiveness in all fields of science. Green synthesized nanomaterials that are mostly used in drug delivery and medical approaches have some downsides to using these metal oxides because of their higher toxicity when used in higher concentrations. All the previous conclusions highlight that there is an actual need for more investigation in order to use CuO-ZnO NPs as encouraging alternate antibacterial materials and anti-cancer therapeutic settings.

Acknowledgment

Many thanks to editor-in-chief and members of the editorial committee in Ibn Al-Haitham Journal for Pure and Applied Sciences.

Conflict of Interest

There are no conflicts of interest.

Funding

There is no funding for the article.

Ethical Clearance

This research was subjected to ethical considerations, and the research was approved by the Committee of Ethical Standards in the college Science, University of Baghdad, in line with the form issued for this purpose by the Iraqi Ministry of Health**.**

References

1. Spirescu, V.A.; Șuhan, R.; Niculescu, A.-G.; Grumezescu, V.; Negut, I.; Holban, A.M.; Oprea, O.-C.; Bîrcă, A.C.; Vasile, B. Ștefan; Grumezescu, A.M. Biofilm-Resistant Nanocoatings Based on ZnO Nanoparticles and Linalool. *Nanomaterials (Basel)* **2021**, *11*, 2564. https://doi.org/10.3390/nano11102564.
2. Balaure, P.C.; Grumezescu, A.M. Recent Advances in Surface Nanoengineering for Biofilm Prevention and Control. Part II: Active, Combined Active and Passive, and Smart Bacteria-Responsive Antibiofilm Nanocoatings. *Nanomaterials (Basel)* **2020**, *10*, 1527, doi:10.339/nano10081527.
3. Kazemzadeh-Narbat, M.; Cheng, H.; Chabok, R.; Alvarez, M.M.; de la Fuente-Nunez, C.; Phillips, K.S.; Khademhosseini, A. Strategies for Antimicrobial Peptide Coatings on Medical Devices: A Review and Regulatory Science Perspective. *Crit. Rev. Biotechnol* **2021**, *41*, 94–120, doi:10.1080/07388551/2020.1828810.
4. Alwash, A. The Green Synthesize of Zinc Oxide Catalyst Using Pomegranate Peels Extract for the Photocatalytic Degradation of Methylene Blue Dye. *Baghdad Sci. J.* **2020**, *17*, 0787, doi:10.21123/bsj.2020.17.3.0787.
5. Mohammed, L.S.; Ahmed, M.E. Effects of ZnO NPS on *Streptococcus pyogenes* in Vivo. *Annals of Tropical Medicine and Public Health* **2020**, *23*, 214–223, DOI:10.36295/ASRO.2020.23228.
6. Jiang, Q.; Chen, J.; Yang, C.; Yin, Y.; Yao, K. Quorum Sensing: A Prospective Therapeutic Target for Bacterial Diseases. *Biomed Res. Int.* **2019**, *2019*, 2015978, doi: 10.1155/2019/2015978.

7. Khalil, A.T.; Ovais, M.; Iqbal, J.; Ali, A.; Ayaz, M.; Abbas, M.; Ahmad, I.; Devkota, H.P. Microbes-Mediated Synthesis Strategies of Metal Nanoparticles and Their Potential Role in Cancer Therapeutics. *Semin. Cancer Biol.* **2022**, *86*, 693–705. DOI: 10.1016/j.semcancer.2021.06.006.
8. Noor, S.; Shah, Z.; Javed, A.; Ali, A.; Hussain, S.B.; Zafar, S.; Ali, H.; Muhammad, S.A. A Fungal Based Synthesis Method for Copper Nanoparticles with the Determination of Anticancer, Antidiabetic and Antibacterial Activities. *J. Microbiol. Methods* **2020**, *174*, 105966. DOI: 10.1016/j.mimet.2020.105966.
9. Ali, M.A.; Ahmed, T.; Wu, W.; Hossain, A.; Hafeez, R.; Islam Masum, M.M.; Wang, Y.; An, Q.; Sun, G.; Li, B. Advancements in Plant and Microbe-Based Synthesis of Metallic Nanoparticles and Their Antimicrobial Activity against Plant Pathogens. *Nanomaterials (Basel)* **2020**, *10*, 1146. DOI: 10.3390/nano10061146.
10. Gajdács, M.; Urbán, E. Comparative Epidemiology and Resistance Trends of Proteae in Urinary Tract Infections of Inpatients and Outpatients: A 10-Year Retrospective Study. *Antibiotics (Basel)* **2019**, *8*, 91. DOI: 10.3390/antibiotics8030091.
11. Jaffar, N.; Miyazaki, T.; Maeda, T. Biofilm Formation of Periodontal Pathogens on Hydroxyapatite Surfaces: Implications for Periodontium Damage: Biofilm Formation of Periodontal Pathogens on Hydroxyapatite Surfaces. *J. Biomed. Mater. Res. A* **2016**, *104*, 2873–2880. DOI: 10.1002/jbm.a.35827.
12. Punniyakotti, P.; Panneerselvam, P.; Perumal, D.; Aruliah, R.; Angaiah, S. Anti-Bacterial and Anti-Biofilm Properties of Green Synthesized Copper Nanoparticles from Cardiospermum Halicacabum Leaf Extract. *Bioprocess Biosyst. Eng.* **2020**, *43*, 1649–1657.DOI: 10.1007/s00449-020-02357-x.
13. Turakhia, B.; Divakara, M.B.; Santosh, M.S.; Shah, S. Green Synthesis of Copper Oxide Nanoparticles: A Promising Approach in the Development of Antibacterial Textiles. *J Coat Technol Res* **2020**, *17*, 531–540, https://doi.org/10.1007/s11998-019-00303-5.
14. Al-Assaf, A.I.S.; Ali, H.M.; Ad'hiah, A.H. Gene Expression of NLRP3 Inflammasome in Celiac Disease of Iraqi Children. *Ibn AL- Haitham J. Pure Appl. Sci.* **2021**, *2021*, 15–22, https://doi.org/10.30526/2021.IHICPAS.2645.
15. Emad, M.; Salama, K. A Comparison of the Effects of Lemon Peel -Silver Nanoparticles versus Brand Toothpastes and Mouthwashes on Staphylococcus Spp. Isolated from Teeth Caries. *Iraqi J. Sci.* **2020**, 1894–1901. DOI: https://doi.org/10.24996/ijs.2020.61.8.6.
16. Kouhkan, M.; Ahangar, P.; Babaganjeh, L.A.; Allahyari-Devin, M. Biosynthesis of Copper Oxide Nanoparticles Using Lactobacillus Casei Subsp. Casei and Its Anticancer and Antibacterial Activities. *Curr. Nanosci.* **2020**, *16*, 101–111, DOI: 10.2174/1573413715666190318155801.
17. Janani, B.; Syed, A.; Raju, L.L.; Al-Harthi, H.F.; Thomas, A.M.; Das, A.; Khan, S.S. Synthesis of Carbon Stabilized Zinc Oxide Nanoparticles and Evaluation of Its Photocatalytic, Antibacterial and Anti-Biofilm Activities. *J. Inorg. Organomet. Polym. Mater.* **2020**, *30*, 2279–2288. https://doi.org/10.1007/s10904-019-01404-9.
18. Al-Jubouri, A.K.; Al-Saadi, N.H.; Kadhim, M.A. Anti-Inflammatory and Anti- Bacterial Activity of Copper Nanoparticles Synthesized from *Myrtus communis* Leaves Extract. *Iraqi J. Agric. Sci.* **2022**, *53*, 698–711, https://doi.org/10.36103/ijas.v53i3.1580.
19. Kang, Q.; Wang, X.; Zhao, J.; Liu, Z.; Ji, F.; Chang, H.; Yang, J.; Hu, S.; Jia, T.; Wang, X. Multidrug-Resistant Proteus Mirabilis Isolates Carrying Bla OXA-1 and Bla NDM-1 from Wildlife in China: Increasing Public Health Risk. *Integr. Zool* **2021**, *16*, 798–809. DOI: 10.1111/1749-4877.12510.
20. Khan, M.F.; Husain, F.M.; Zia, Q.; Ahmad, E.; Jamal, A.; Alaidarous, M.; Banawas, S.; Alam, M.M.; Alshehri, B.A.; Jameel, M. Anti-Quorum Sensing and Anti-Biofilm Activity

of Zinc Oxide Nanospikes. *ACS Omega* **2020**, *5*, 32203–32215, doi: 10.1021/acsomega.0c03634.

21. Siddiqi, K.S.; ur Rahman, A.; Tajuddin; Husen, A. Properties of Zinc Oxide Nanoparticles and Their Activity against Microbes. *Nanoscale Res. Lett.* **2018**, *13*, 141. https://doi.org/10.1186/s11671-018-2532-3.
22. Hasson, S.O.; Salman, S.A.K.; Hassan, S.F.; Abbas, S.M. Antimicrobial Effect of Eco- Friendly Silver Nanoparticles Synthesis by Iraqi Date Palm (*Phoenix dactylifera*) on Gram-Negative Biofilm-Forming Bacteria. *Baghdad Sci. J.* **2021**, *18*, 1149, DOI: https://doi.org/10.21123/bsj.2021.18.4.1149.
23. Ahmed, M.E.; Al-Shimmary, S.M. Comparative Study between Pure Bacterocin and Vancomycin on Biofilms of MRSA Isolated from Medical Implants. *Journal of Pharmaceutical Sciences and Research*, **2018**, *10*, 1476–1480.
24. Bondarenko, O.M.; Sihtmäe, M.; Kuzmičiova, J.; Ragelienė, L.; Kahru, A.; Daugelavičius, R. Plasma Membrane Is the Target of Rapid Antibacterial Action of Silver Nanoparticles in *Escherichia coli* and *Pseudomonas aeruginosa*. *Int. J. Nanomedicine* **2018**, *13*, 6779–6790. DOI: 10.2147/IJN.S177163.
25. Hussein, E.I.; Al-Batayneh, K.; Masadeh, M.M.; Dahadhah, F.W.; Al Zoubi, M.S.; Aljabali, A.A.; Alzoubi, K.H. Assessment of Pathogenic Potential, Virulent Genes Profile, and Antibiotic Susceptibility of *Proteus mirabilis* from Urinary Tract Infection. *Int. J. Microbiol.* **2020**, *2020*, 1231807. https://doi.org/10.1155/2020/1231807.
26. Rajalakshmi, R.; Sangeetha, D.; Udhaya, V. Effect of Antifungal Drugs against *Candida* Isolates from Diabetic Women with Vaginitis. *J. Infect. Dis. Ther* **2017**, *5*, 331. doi: 10.4172/2332-0877.1000331.
27. Mishu, J.; Sm, N.; Hm, S.; Nabonee, K.; Zannat Dola, M.A.; Haque, N. Association between Biofilm Formation and Virulence Genes Expression and Antibiotic Resistance Pattern in Proteus Mirabilis, Isolated from Patients of Dhaka Medical College Hospital. *Arch. Clin. Biomed. Res*. **2022**, 6, 3, 418-434. DOI: 10.26502/acbr.50170257.
28. Badawy, M.S.E.M.; Riad, O.K.M.; Taher, F.A.; Zaki, S.A. Chitosan and Chitosan-Zinc Oxide Nanocomposite Inhibit Expression of *LasI* and *RhlI* Genes and Quorum Sensing Dependent Virulence Factors of *Pseudomonas aeruginosa*. *Int. J. Biol. Macromol*. **2020**, *149*, 1109–1117, DOI: 10.1016/j.ijbiomac.2020.02.019.
29. Abdul-Hamza, H.K.; Mohammed, G.J. Anti-Quorum Sensing Effect of Streptococcus Agalatiaceae by Zinc Oxide, Copper Oxide, and Titanium Oxide Nanoparticles. *J. Phys. Conf. Ser*. **2021**, *1999*, 012031, https://iopscience.iop.org/article/10.1088/1742-6596/1999/1/012031.
30. Cai, X.; Liu, X.; Jiang, J.; Gao, M.; Wang, W.; Zheng, H.; Xu, S.; Li, R. Molecular Mechanisms, Characterization Methods, and Utilities of Nanoparticle Biotransformation in Nanosafety Assessments. *Small* **2020**,*16*, e1907663, https://doi.org/10.1002/smll.201907663.
31. Ram, V.P.; Rao, L.V.; Rao, T.S.; Subramanyam, K.V.; Suresh, Y.; Srinivas, K. A Study on Antibiogram and Beta-Lactam Resistance of Proteus Mirabilis Isolated from Animals and Humans in Andhra Pradesh, India. *Indian J. Anim. Res.* **2021**, doi: 10.18805/IJAR.B-4184.
32. Alavi, M.; Li, L.; Nokhodchi, A. Metal, Metal Oxide and Polymeric Nanoformulations for the Inhibition of Bacterial Quorum Sensing. *Drug Discov. Today* **2023**, *28*, 103392. DOI: 10.1016/j.drudis.2022.103392.
33. Yao, Y.; Zhou, Y.; Liu, L.; Xu, Y.; Chen, Q.; Wang, Y.; Wu, S.; Deng, Y.; Zhang, J.; Shao, A. Nanoparticle-Based Drug Delivery in Cancer Therapy and Its Role in Overcoming Drug Resistance. *Front. Mol. Biosci.* **2020**, *7*, DOI: 10.3389/fmolb.2020.00193.
34. Reddy, K.M.; Feris, K.; Bell, J.; Wingett, D.G.; Hanley, C.; Punnoose, A. Selective Toxicity of Zinc Oxide Nanoparticles to Prokaryotic and Eukaryotic Systems. *Appl. Phys. Lett.* **2007**, *90*, 2139021–2139023. doi: 10.1063/1.2742324.
35. Kang, Q.; Wang, X.; Zhao, J.; Liu, Z.; Ji, F.; Chang, H.; Yang, J.; Hu, S.; Jia, T.; Wang, X. Multidrug-Resistant Proteus Mirabilis Isolates Carrying blaOXA-1 and blaNDM-1 from Wildlife in

China: Increasing Public Health Risk. *Integr. Zool.* **2021**, *16*, 798–809. DOI: 10.1111/1749-4877.12510.

36. Ameh, T.; Sayes, C.M. The Potential Exposure and Hazards of Copper Nanoparticles: A Review. *Environ. Toxicol. Pharmacol.* **2019**, *71*, 103220. DOI: 10.1016/j.etap.2019.103220.
37. Abbasi, A.; Ghorban, K.; Nojoomi, F.; Dadmanesh, M. Smaller Copper Oxide Nanoparticles Have More Biological Effects versus Breast Cancer and Nosocomial Infections Bacteria. Asian Pac. *J. Cancer Prev* **2021**, *22*, 893–902. DOI: 10.31557/APJCP.2021.22.3.893.
38. Haupenthal, D.P.D.S.; Possato, J.C.; Zaccaron, R.P.; Mendes, C.; Rodrigues, M.S.; Nesi, R.T.; Pinho, R.A.; Feuser, P.E.; Machado-de-Ávila, R.A.; Comim, C.M. Effects of Chronic Treatment with Gold Nanoparticles on Inflammatory Responses and Oxidative Stress in Mdx Mice. *J. Drug Target.* **2020**, *28*, 46–54. DOI: 10.1080/1061186X.2019.1613408.
39. Ali, K.H.; Ibraheem, S.A.; Jabir, M.S.; Ali, K.A.; Taqi, Z.J.; Dan, F.D. Zinc Oxide Nanoparticles Induces Apoptosis in Human Breast Cancer Cells via Caspase-8 and P53 Pathway. *Nano Biomed. Eng.* **2019**, *11*, 35-43. https://doi.org/10.5101/nbe.v11i1.p35-43.
40. Rashid, A.E.; Ahmed, M.E.; Hamid, M.K. Evaluation of Antibacterial and Cytotoxicity Properties of Zinc Oxide Nanoparticles Synthesized by Precipitation Method against Methicillin-Resistant *Staphylococcus aureus*. *Int. J. Drug Deliv. Technol.* **2022**, *12*, 985–989. DOI:10.25258/ijddt.12.3.11.
41. Hassan, Z.J.S.; Hamid, M.K.; Ahmed, M.E. Synthesized Zinc Oxide Nanoparticles by the Precipitation Method on *Streptococcus* spp. from Dental Carries and Cytotoxicity Assay. *Int. J. Drug Deliv. Technol.* **2022**, *12*, 1327–1330. DOI: 10.25258/ijddt.12.3.65.
42. Mani, V.M.; Kalaivani, S.; Sabarathinam, S.; Vasuki, M.; Soundari, A.J.P.G.; Ayyappa Das, M.P.; Elfasakhany, A.; Pugazhendhi, A. Copper Oxide Nanoparticles Synthesized from an Endophytic Fungus *Aspergillus terreus*: Bioactivity and Anti-Cancer Evaluations. *Environ. Res.* **2021**, *201*, 111502. DOI: 10.1016/j.envres.2021.111502.